Nuclear Instruments and Methods in Physics Research B 538 (2023) 41–46

Contents lists available at ScienceDirect

Nuclear Inst. and Methods in Physics Research, B

journal homepage: www.elsevier.com/locate/nimb

Deuterium and helium retention in W and W-Ta coatings irradiated with energetic ion beams

R. Mateus [a,*], N. Catarino [a], M. Dias [a], L.C. Alves [b], O. Romanenko [c], Z. Siketić [d], I. Bogdanović Radović [d], A. Hakola [e], E. Grigore [f], E. Alves [a], WP PFC contributors[a,1]

[a] IPFN, Instituto Superior Técnico, Universidade de Lisboa, 2695-066 Bobadela, Portugal
[b] C2TN, Instituto Superior Técnico, Universidade de Lisboa, 2695-066 Bobadela, Portugal
[c] Czech Academy of Sciences, Nuclear Physics Institute, Hlavni 130, Řež 25068, Czech Republic
[d] Ruđer Bošković Institute, P.O. Box 180, 10002 Zagreb, Croatia
[e] VTT Technical Research Centre of Finland Ltd, P. O. Box 1000, 02044 VTT, Finland
[f] National Institute for Lasers, Plasma and Radiation Physics, 077125 Bucharest, Romania

ARTICLE INFO

Keywords:
W-Ta coatings
Helium
Deuterium
Retention

ABSTRACT

Different studies reveal the behaviour of Ta alloying to decrease deuterium retention in tungsten bulk materials aiming to be used for nuclear fusion applications. In this work, W and W-5 %Ta coatings were produced via magnetron sputtering techniques. The elemental composition of the samples and the spread of Ta in the W lattice was confirmed by GDOES, PIXE and by μ-PIXE, respectively. Sets of W and W-Ta coatings were simultaneously irradiated with a single $^2H_2^+$ or with sequential $^4He^+/^2H_2^+$ ion beam implantations using incident energies of 30 keV and ion fluences of 5×10^{17} ion/cm^2. The irradiated samples were analysed by NRA/RBS and by ToF-ERDA to quantify the retained deuterium and helium amounts. The results reveal significantly lower contents of both isotopes in W-Ta.

1. Introduction

Tungsten (W) is foreseen to be the main material for plasma facing applications in fusion devices due to its low neutron activation, superior thermal–mechanical properties [1,2] and low hydrogen solubility [2]. Even so, difficulties persist due to the ductile-to-brittle transition temperature (DBTT) of the existing W-based materials [1,2], leading to reduced ductility at low operation temperatures. Tantalum (Ta) exhibits higher ductility and radiation resistance than W [1–4] as well as low neutron activation. In addition, it transmutes to W under neutron irradiation and forms complete solid solutions with W [4]. The addition of low contents of Ta in the W lattice is under investigation as a natural approach to improve the properties of W bulk materials. Nominal content of 5 % of Ta, W-5 %Ta, is here used as a standard composition for the investigations [1,2]. In parallel to bulk materials, W coatings are produced to cover the first walls of experimental tokamaks [5], which justifies the development of coating alloys for similar purposes.

The radiation resistance and the retention of deuterium (^{2}H) in the alloys is being investigated with low energy plasma irradiations (of few eV) [2,6]. On the other hand, implantation experiments with incident ion energies of few MeV are also suggested for the investigations [1]. Besides irradiations within the eV and MeV energy ranges, ion beams of 10–100 keV are widely used, while they are able to impose huge modifications with moderate ion fluences along the implantation zone near the superficial layers [7,8]. Even so, previous irradiation experiments performed with incident 30 keV $^4He^+$ beams in polycrystalline tungsten at elevated temperatures have shown that extreme structural changes occur when ion fluences exceed the threshold level of 1×10^{18} ions/cm^2, promoting helium (He) release through nano-channels formed by the coalescence and movement of He bubbles [8]. In order to prevent these effects and to compare the behaviour of the materials to retain deuterium and helium, a simple irradiation campaign was carried out at room temperature (RT) using energetic $^2H_2^+$ (molecular deuterium) and $^4He^+$ ion beams at significantly lower ion fluences, i.e., 5×10^{17} ion/cm^2.

2. Experiment

W and Ta metallic sources of high purity (99.98 %) were positioned

* Corresponding author.
E-mail address: rmateus@ipfn.tecnico.ulisboa.pt (R. Mateus).
[1] See the author list in "S. Brezinsek et al., Nucl. Fusion 57 (2017) 116041."

https://doi.org/10.1016/j.nimb.2023.02.028
Received 28 November 2022; Received in revised form 16 January 2023; Accepted 21 February 2023
Available online 1 March 2023

Table 1
Quantified ^{4}He and ^{2}H contents: along the total integration depth (implantation zone plus diffusion zone) or only in the implantation zone [square brackets].

Coating	Irradiation		ToF-ERDA		NRA
	$^4He^+$	$^2H_2^+$	^{4}He content (10^{17} at./cm^2)	^{2}H content (10^{17} at./cm^2)	^{2}H content (10^{17} at./cm^2)
W	–	30 keV $^2H_2^+$			1.62 [1.11][d]
W	30 keV $^4He^+$	30 keV $^2H_2^+$	3.64 [3.03][a]	2.29 [1.94][b]	3.27 [2.52][c]
W-5%Ta	–	30 keV $^2H_2^+$			0.92 [0.74][h]
W-5%Ta	30 keV $^4He^+$	30 keV $^2H_2^+$	2.10 [1.73][e]	1.24 [1.09][f]	1.56 [1.44][g]

Integration depths of ~20 × 10^{18} at./cm^2 for NRA, and of ~3 × 10^{18} at./cm^2 for ToF-ERDA analyses. Ion fluences of 5 × 10^{17} ion/cm^2 in all the irradiations, i.e., the retention rates at the implantation zone are: 0.61[a], 0.39[b], 0.50[c], 0.22[d] in W; 0.35[e], 0.22[f], 0.29[g], 0.15[h] in W-Ta.

in two independent magnetron sputtering setups energized separately in order to adjust the deposition parameters to obtain the desired nominal compositions for the coatings, i.e., pure W and W-5 %Ta (95 at.% of W, 5 at.% of Ta), and thicknesses of the deposits close to ~6 μm. W deposition was carried out via Direct Current Magnetron Sputtering (DCMS) with a target current of 0.3 A (total power of 135 W). Ta deposition, for its part, was carried out via High Power Impulse Magnetron Sputtering (HiPIMS) with a target voltage amplitude of −1 kV, being the average power discharges tuned for a bias frequency of 4.3 Hz (pulsed regime) [9]. An Ar atmosphere was used as working gas at a base pressure of 4.1 × 10^{-3} mbar (Ar mass flow rate of 9.0 sccm). The magnetron sputtering cathodes and the sampler holder were positioned in a confocal geometry inside the deposition chamber assuring that uniform W and Ta fluxes reach the substrates. Molybdenum (Mo) (15 × 12 × 1 mm) and titanium (Ti) substrates were used simultaneously: Mo samples for the irradiation experiments and Ti samples as witness coatings to quantify the deposited elemental depth profiles by Glow Discharge Optical Emission Spectrometer (GDOES). GDOES was done with a Spectruma GDA 750 analyser, enabling a spatial resolution of 0.025 nm in the spectral range 190–800 nm [10]. The particular analysis of W and Ta depth profiles by GDOES was achieved from the corresponding emission lines at 429.46 nm and at 362.66 nm, respectively. Additional details about the deposition procedure and DCMS, HiPIMS and GDOES setups are presented elsewhere [9,10].

In order to investigate the elemental composition of the produced coatings with possible impurity quantification, Proton Induced X-ray Emission (PIXE) measurements were performed with a broad ion beam of 1 mm of diameter and with an ion beam microprobe (μ-PIXE) assuring a cross-sectional spot size of ~3 × 4 μm^2. PIXE allows quantification of elemental concentrations for all elements heavier than sodium (Na) down to the ppm range. Broad beam measurements were performed with 2300 keV $^1H^+$ ions using a Mylar foil of 50 μm in front of a Si(Li) detector to absorb intensive W and Ta M X-ray lines. W and Ta contents were quantified by analysing the W-Lα and Ta-Lα line yields in the X-ray spectra (8.40 keV and 8.15 keV, respectively) with the GUPIX code [11]. The homogeneity of the W-Ta films was evaluated by μ-PIXE using 2000 keV $^1H^+$ ions, a 350 μm absorber foil and a Si drift detector. Microbeam data analysis was done using the OMDAQ software [12]. Aiming to avoid the superposition of the X-ray peak yields, independent elemental mapping for W and Ta was performed by selecting the W-Lα and Ta-Lγ_1 lines (8.40 keV and 10.90 keV, respectively) collected from scanned areas ranging from 1320 × 1320 μm^2 down to 106 × 106 μm^2. Afterwards, the role of Ta addition in the retention behaviour of deuterium and helium was investigated following an ion implantation experiment carried out with a 210 keV high flux ion implanter by impinging energetic deuterium and helium ion beams at RT with normal incidence to the target surfaces. A first set composed by a W and a W-Ta coating deposited on Mo was irradiated with a single ion implantation using a 30 keV $^2H_2^+$ ion beam (30 keV molecular deuterium ions; 15 keV by incident ^{2}H nuclei) with a fluence of 5 × 10^{17} ion/cm^2. A second and similar set of coatings was irradiated with a sequential ion implantation in two consecutive steps: the first one using an incident 30 keV $^4He^+$ beam with the same fluence of 5 × 10^{17} ion/cm^2; the second one using the previous incident 30 keV $^2H_2^+$ beam with the ion fluence of 5 × 10^{17} ion/cm^2. For the ion implantation operation, the ion beam spot with a transverse cross-section of ~1 cm^2 was scanned along an area of ~30 × 50 mm^2, irradiating homogeneously and simultaneously the entire W and W-Ta coating's surfaces. The current densities were maintained at ~10 μA/cm^2, leading to ion fluxes and sample temperatures lower than 1.5 × 10^{14} ion/(cm^2·s) and 50 °C during irradiation, respectively. The scheme of the entire ion implantation experiment is shown in Table 1 (see Section 3). The irradiation experiment took into consideration the in-depth ranges achieved by both ion species along the depth of a pure W layer as calculated by the SRIM code [7]. Corresponding irradiation damages induced by single 15 keV $^2H^+$ or 30 keV $^4He^+$ implantation in pure W was also evaluated by SRIM using the "quick Kinchin-Pease" calculation option, a displacement energy of 90 eV and a lattice binding energy of 0 eV for vacancy formation in bulk W [13], and an atomic density of 6.34 × 10^{22} at./cm^2 for W [7]. Both secondary atomic W recoils and direct W displacements imposed by ion knock-ons were considered to calculate the damage dose [13]. SRIM results achieved for pure W were used to evaluate irradiation effects in both W and W-Ta coatings, while the addition of 5 at.% of Ta in the W lattice leads to negligible changes in the final material density and in the energy losses imposed to incident ions.

Irradiated coatings were simultaneously analysed by Nuclear Reaction Analysis (NRA) to quantify retained deuterium contents down to a deep depth by following the p_0 emission yields of the $^2H(^3He,p_0)^4He$ reaction and by Rutherford Backscattering (RBS) to normalize the $^2H(^3He,p_0)^4He$ yields in the NRA spectra, using incident 2300 keV and 1250 $^3He^+$ ion beams, a passivated implanted planar silicon detector placed at an angle of 140° to the incident $^3He^+$ beam direction for the NRA analysis and a second particle detector for the RBS analysis placed at a scattering angle of 165°. Channel-to-energy calibration of the NRA spectra as well as the check of the detection geometry was performed with the analysis of a pure thick Be sample at the same experimental conditions, taking advantage of the collected $^9Be(^3He,p_i)^{11}B$ reaction yields [14]. For this purpose, a 75 μm thick Mylar foil was positioned in front of the NRA detector to absorb energetic α particles emitted from Be. RBS and NRA spectra were analysed with the NDF code [15]. Additionally, Time-of-Flight Elastic Recoil Detection (ToF-ERDA) using a 23 MeV $^{127}I^{6+}$ ion beam impinging on the targets at a glancing angle of 20° and a gas ionisation detector positioned at an angle of 37.5° toward the beam direction [16] was performed. The analysis enables to quantify simultaneously the retained amounts of both implanted isotopes, deuterium and helium, and also the presence of light contaminants as hydrogen (^{1}H), carbon (^{12}C) or oxygen (^{16}O). Spectra analysis was carried out with the POTKU software [17], checking possible modification effects imposed by $^{127}I^{6+}$ ion bombardment to light element composition. Eventual morphological modifications induced by irradiation at the samples surface were evaluated by Scanning Electron Microscopy (SEM). As in the case of PIXE, NRA, RBS and ToF-ERDA measurements, SEM analysis was performed nearby the central zone of the coatings.

3. Results and discussion

The temperature of the substrates and coatings was maintained at ~200 °C, as result of the heating effect generated by plasma radiation, by keeping the same plasma parameters during the sputter deposition. The microstructure of the coatings depends of the sample's temperature. The experience evidence that columnar grows are induced for deposition temperatures in the range 150–400 °C. Therefore, and as a consequence of the heating procedure, both W and W-Ta coatings exhibit a typical columnar microstructure, as observed by SEM inspection [5]. The maintenance of the optimized plasma parameters also assures the desired stoichiometry of the W-Ta samples, i.e., W-5 %Ta. Fig. 1 presents the elemental depth profiles of a control W-Ta witness coating deposited on Ti achieved by GDOES. A slight carbon (C) contamination is present at the surface and at the interface layer with the Ti substrate. C contamination is due to the exposure in air in the period elapsed from deposition till the GDOES measurement, which, in turn is tuned to evidence the gathering of C with high sensitivity. Therefore, the GDOES yield for C is overrated. A tailored Ta composition of ~5 at.% was quantified along the depth of the coating, with a thickness close to ~6.5 μm. The error for the Ta quantification by GDOES was ~12 %. Apart the absence of Ta, W coatings exhibit similar depth profiles. W and Ta co-deposition in the Mo substrates and the spread of Ta in the W lattice is also confirmed with the W and Ta elemental maps obtained by μ-PIXE. From the analysis of the 530 × 530 μm^2 W and Ta maps shown in Fig. 2 (a) and (b), respectively, it can be concluded that the composition of the W-Ta layer is homogeneous down to a beam lateral resolution of ~3x4 μm^2 (the cross-section spot size). The same homogeneous behaviour is achieved from the analysis of all the scanned areas. Ta contents of 6.1 at. % were always quantified by μ-PIXE. Aiming at a broad elemental analysis of the central zone of the coatings surface, broad beam PIXE spectra were also collected from the W and W-Ta samples. Fig. 2(c) presents one of the W-Ta spectra and the most intense X-ray lines arising from W-L and Ta-L emissions. Apart W and Ta, only the Mo-K lines achieved from the Mo substrate are visible. Impurities heavier than Na are inexistent or at the level of few ppm. As in the case of μ-PIXE, Ta concentrations of 6.1 at.% were always quantified by PIXE in the W-Ta films with the same error quantification of ~0.5 at.%. X-ray analysis is more sensitive at the superficial layers. Also, a slight superficial peak is observed for the Ta content in the GDOES depth profile. Therefore, we may affirm that PIXE and GDOES quantifications for the Ta amounts are compatible (6.1 ± 0.5 at.% and 5.0 ± 0.6 at.%, respectively). Apart from the absence of Ta, similar results were obtained from the analysis of W samples by PIXE.

SRIM simulations show superposition of both $^4He^+$ and $^2H_2^+$ ion depth ranges along the implantation zone in a W layer: depth ranges (Rp) of 78 and 88 nm, with straggling ranges (ΔRp) of 38 and 44 nm, for the normal incidence of 30 keV $^4He^+$ and 15 keV $^2H^+$ in pure W, respectively [7]. Ion range depth profiles are presented in Fig. 3. Almost all incident ions become retained within a 150–200 nm implantation depth. High atomic fractions are achieved for both retained isotopes after irradiation with operated fluences of 5 × 10^{17} ion/cm^2, showing that irradiation campaigns with energetic ions may impose extreme irradiation effects to the materials with moderated fluences. Obviously, part of the implanted ions will not be held in the bulk lattice but in grain boundaries (GBs), leading to high mobility [18]. Fig. 3 also present the simulated irradiation damage imposed by $^4He^+$ and by $^2H^+$ exposure at the same fluences, showing that induced defects are spread shallower comparing to ion depth ranges where most of incident ion energy is transmitted to the W lattice (maximum irradiation damage induced by ^4He and ^2H ions lies at a depth of ~45 nm). As predicted [3,4,7], induced irradiation effects are widely enhanced after helium implantation and remain quite negligible when deuterium exposure occurs. Retention tends to occur in lattice defects [18]. From the simulated ion depth range and damage profiles we may expect an enhanced helium and deuterium retention behaviour along the first 150–200 nm for both W and W-Ta materials (down to a depth of ~1250 × 10^{15} at./cm^2 in pure W), while atomic diffusion towards the bulk material is hampered by superficial damage [18].

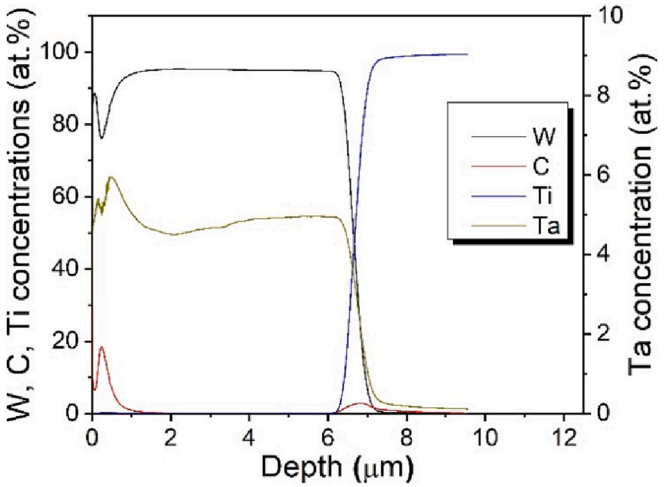

Fig. 1. Elemental depth profiles of W-Ta coatings achieved by GDOES [10].

Fig. 4 shows the depth profiles of retained deuterium quantified by NRA in the W and W-Ta coatings after irradiation. Most of the retained amounts are spread within the same superficial depth zone, and at deeper depths lower amounts of deuterium still exist. According to SRIM simulations, an implantation zone and a diffusion zone is identified. NRA analysis provides a good sensitivity for deuterium quantification down to the depth limit range of the technique (~20 × 10^{18} at./cm^2 in the present samples, i.e., 3.0–3.5 μm). Nevertheless, the depth sensitivity is also limited by the low energy resolution of NRA (~100 keV in the present experiment). Therefore, Fig. 4 only presents average contents quantified for deuterium in both implanted and diffusion depth ranges. Distinct retention behaviours are easily revealed in both materials. After single $^2H^+$ and sequential $^4He^+/^2H^+$ irradiation of the W coating, the quantified deuterium contents are ~2.3 at.% and ~5.4 at.% at the implantation zone along a depth range down to ~4700 × 10^{15} at./cm^2, and decrease to ~3.5 × 10^{-1} at.% and ~0.5 at.% at the diffusion zone down to the depth limit of the NRA analysis (~20 × 10^{18} at./cm^2), respectively. Corresponding deuterium amounts are significantly lower in the irradiated W-Ta. They are ~1.3 at.% and ~3 at.% inside the implantation zone under single $^2H^+$ and sequential $^4He^+/^2H^+$ irradiation, respectively, and they strongly decrease at deeper depths, ~0.1 at. %. In all the NRA spectra, the $^2H(^3He,p_0)^4He$ yields remain extended down to the depth limit of the NRA technique, confirming that diffused deuterium still exists beyond the NRA depth limit range. This behaviour is known for W materials and agrees with irradiation data previously reported [19].

Opposite to the limited depth resolution of NRA, ToF-ERDA analysis is very sensitive to changes in the elemental depth contents along the superficial layers. W and W-Ta coatings exposed to the sequential $^4He^+/^2H^+$ irradiation were analysed by ToF-ERDA. The quantified depth profiles for the existing light isotopes in the irradiated W and W-Ta coatings are presented in Fig. 5(a) and (b), respectively, i.e., hydrogen ^1H, ^2H, ^4He, carbon ^{12}C and oxygen ^{16}O. The statistics of the ToF-ERDA data was limited by a significant noise caused by the analysis of heavy matrixes and by the time needed to perform the measurements. Even so, changes in the isotopic yields were not observed with irradiation time, meaning that elemental loss imposed by $^{127}I^{6+}$ irradiation is not an error source in the analysis, particularly for helium and hydrogen quantification. Apart a thin superficial layer (down to ~250 × 10^{15} at./cm^2), light impurity contents are lower than 1–2 at.%. A higher O content in W-Ta superficial layers is justified by the affinity of Ta to react with

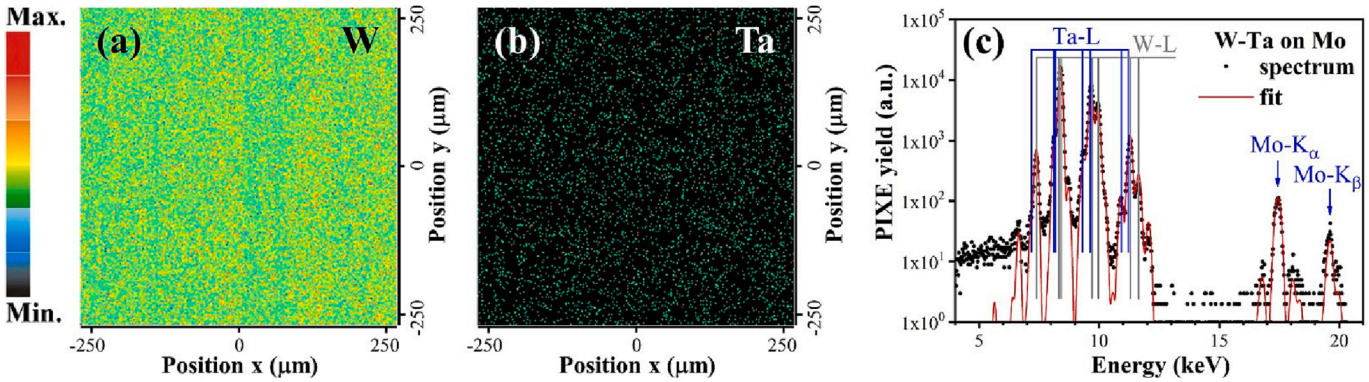

Fig. 2. μ-PIXE analysis of an as-deposited W-Ta coating using a 2.0 MeV $^{1}H^{+}$ beam: homogeneous distribution of Ta in W; 530 × 530 μm^2 maps for the W-Lα (a) and Ta-Lγ_1 X-ray yields (b) [12]. Broad beam PIXE spectra collected with an incident 2.3 MeV $^{1}H^{+}$ beam with W-L, Ta-L and Mo-K peaks and corresponding fit line arising from the elemental analysis [11](c).

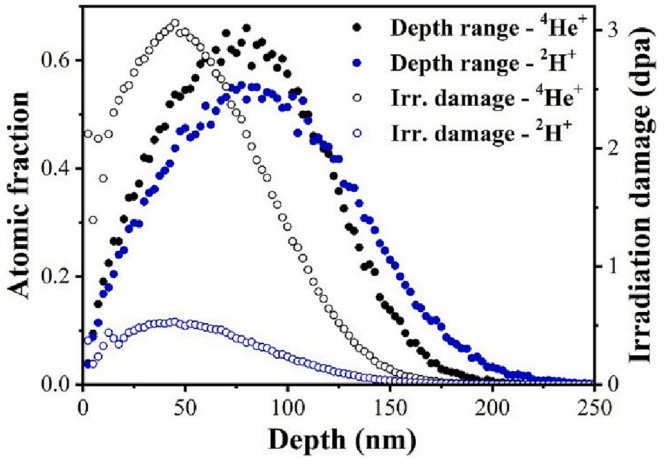

Fig. 3. Ion range and damage depth profiles imposed by $^{4}He^{+}$ and $^{2}H^{+}$ irradiation in pure W (incident energies of 30 keV; fluences of 5 × 10^{17} ion/cm^2) [7].

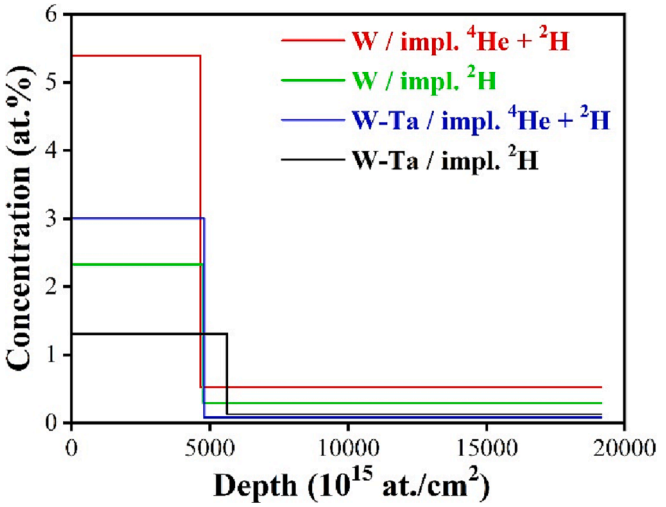

Fig. 4. Deuterium depth profiles in irradiated W and W-Ta coatings quantified by NRA [15].

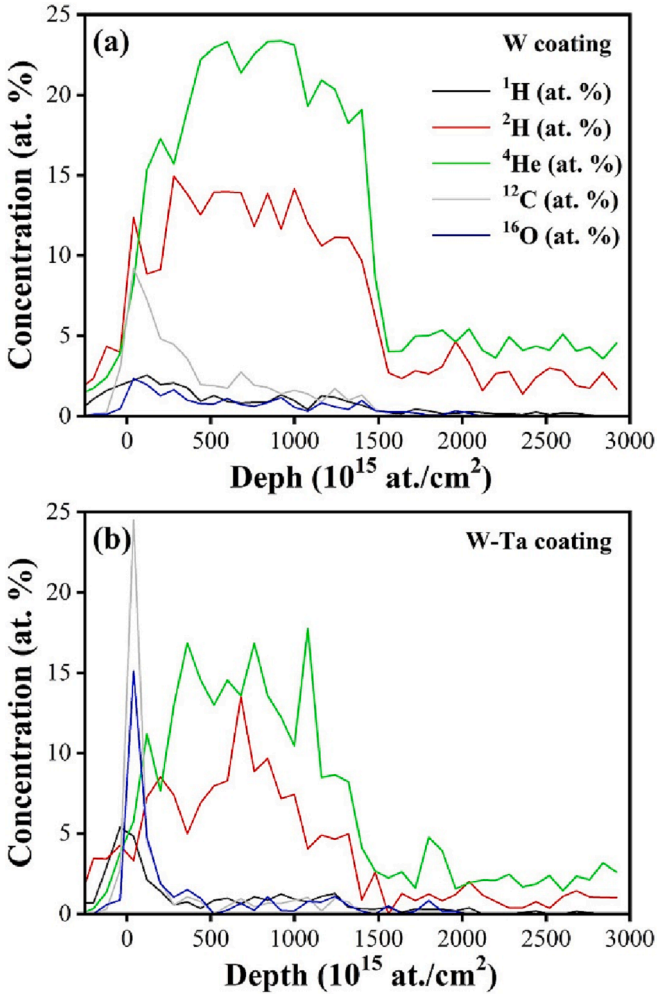

Fig. 5. ToF-ERDA depth profiles of light elements [17]: W (a) and W-Ta (b) coatings implanted by $^{4}He^{+}$ and $^{2}H_2^{+}$.

oxygen [3,4], and C is also present, as already observed in the GDOES elemental depth profile (Fig. 1). However, it does not influence the global analysis, while helium and deuterium are spread down to the coating depth. SRIM simulations point to maximum depth ranges of 200 nm for the implanted $^{4}He^{+}$ and $^{2}H^{+}$ ions in bulk W, which is equivalent to a thickness close to 1250 × 10^{15} at./cm^2 for W (compare Figs. 3 and 5). ToF-ERDA results exhibit superficial layers widely enriched by ^{4}He and ^{2}H with thicknesses close to 1500 × 10^{15} at./cm^2 for both W and W-Ta samples (Fig. 5). The result agrees with the huge ^{4}He and ^{2}H contents and ion ranges achieved in SRIM simulations (Fig. 3). The effect of

irradiation damage promoting ion retention near the superficial layers leads to the huge gathering of helium and deuterium atoms, and to an increase in the thickness of the implantation zone. Helium and deuterium reach the saturation threshold within the implantation zone and easily diffuse towards the lattice bulk in face of relatively low migration energies for light helium and deuterium in W, particularly along GBs [18]. The diffusion effect is observed in the ToF-ERDA profiles at larger depths beyond 1500 × 10^{15} at./cm^2, where the helium and deuterium yields strongly decrease. As in the case of the NRA analytical results for deuterium, also helium and deuterium amounts quantified by ToF-ERDA are significantly lower in the W-Ta coating in both implantation zone and diffusion zone.

Fig. 6(a) presents a SEM image of the W coating surface after irradiation by helium and deuterium ion beams, revealing a rough and faceted morphology, imposing the broadening of the C depth profile towards deeper depths, as achieved by ToF-ERDA, due to the grazing geometry of the ToF-ERDA setup. The same trend is observed from the ^{1}H and O profiles in Fig. 5(a). In opposition, surface roughness is widely reduced in the W-Ta coating, as revealed by Fig. 6(b). As a consequence, it is observed a strong superficial peak in the C depth profile in Fig. 5(b), while C content is reduced at deeper depths. Similar morphologies were observed from the as-deposited coatings. Together with SEM images, ToF-ERDA analysis reveals a C contamination restricted to the superficial layers, with negligible influence in the retained deuterium amounts along the implantation and diffusion zones.

Helium and deuterium contents retained in the irradiated W and W-Ta coatings, as quantified by NRA and by ToF-ERDA, are presented in Table 1 and fully agree with each other, while the depth range limit of the individual analyses is distinct and higher for NRA (~20 × 10^{18} at./cm^2 vs ~3 × 10^{18} at./cm^2, respectively), meaning that NRA retention values for deuterium will be higher than those of ToF-ERDA. In opposition, ToF-ERDA enables a high sensitivity for elemental depth profiling at the superficial layers. The whole analysis reveals that most of deuterium and helium is retained nearby the superficial layers within the implantation zone, as predicted by SRIM. For a single ^{2}H$^+$ and also for a sequential ^{4}He$^+$/^{2} H$^+$ irradiation, the addition of 5 at.% of Ta in the W lattice led to the decrease of the retained deuterium and helium amounts by a factor of ~1.90, as quantified by NRA and by ToF-ERDA. Similar conclusions arise from the analysis of the retained amounts within the implantation zone (see the square brackets in Table 1), while deuterium and helium retention (and the corresponding retention rates, also presented in the notes of Table 1) decrease by a factor of ~1.70 in W-Ta relative to W. All the results point to a significant decrease of the retention behaviour in W-Ta. Errors for the elemental quantifications presented in Table 1 are of the order of 5 % for the case of NRA data (statistical errors, mainly) and 6–7 % for the case of ToF-ERDA data (statistical plus stopping power errors). It is known that Ta addition enhances solid solution strengthening and radiation resistance, and it decreases the unit cell parameters of W alloys produced by powder metallurgy and sintering [1,2], which may justify a better performance of W-Ta alloys under irradiation. We may speculate that similar features could be revealed by the present coatings.

The experience in the research team evidence that the irradiation of bulk W with 30 keV ^{4}He$^+$ ions at RT with a fluence limited to 5 × 10^{17} ion/cm^2, followed by ^{2}H$^+$ irradiation at similar RT and fluences, do not induce the blistering of the surfaces [3,4]. Only a slight swelling of W along grain boundaries occurs [3,4], which obviously reveals the beginning of the blistering mechanisms in zones with higher crystalline defect densities. These morphological modifications are difficult to observed by SEM in the present work, while the irradiated surfaces present irregular and faceted morphologies [5], hampering most of the eventual structural changes imposed by the irradiation campaign [8]. The result also reveals advantages on the use of the operated fluences in the present work, in order to avoid deuterium and helium release.

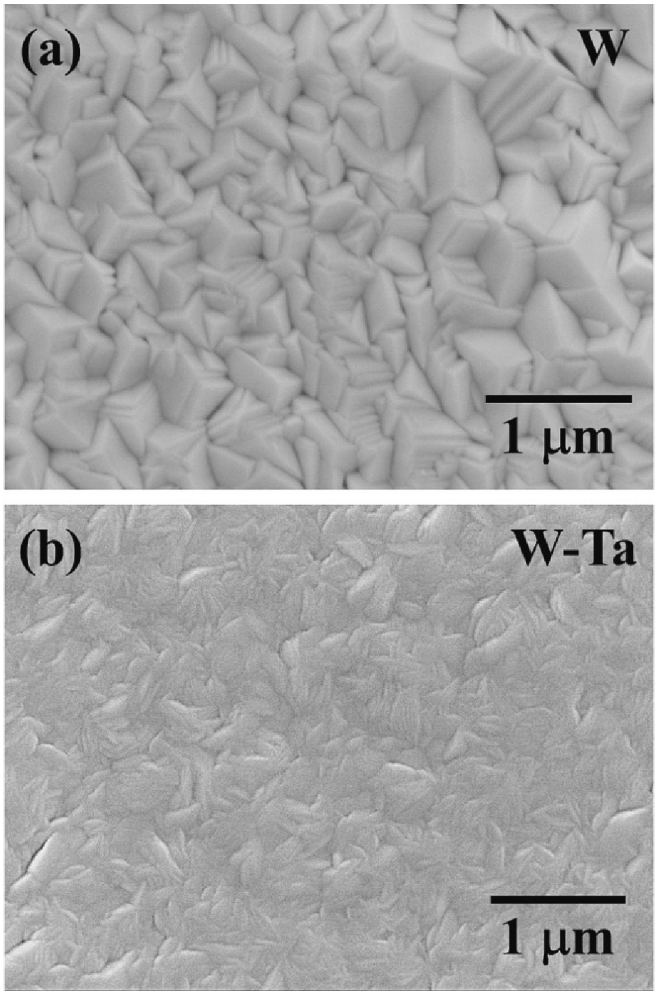

Fig. 6. SEM images (top views) of the W and W-Ta coating surfaces after ^{4}He$^+$ and ^{2}H$_2^+$ irradiation.

4. Summary

W and W-5 %Ta coatings were deposited by DCMS and HiPIMS with a tuned composition of 5 at.% for Ta, as controlled by GDOES analysis. The elemental composition of the samples and elemental homogeneity of the W-Ta coatings were confirmed by PIXE and by μ-PIXE, respectively. After implantation with energetic deuterium ions significantly lower amounts of deuterium became retained in W-Ta relatively to pure W. Lattice defects are highly enhanced by helium irradiation and therefore, a pre-irradiation with energetic helium ions, followed by a second irradiation with deuterium ions was also performed to both W and W-Ta, revealing significantly lower retained helium and deuterium amounts in the W-Ta coating. In order to enhance the irradiation effects and avoid a significant release of retained atoms, all the irradiations were performed with incident energies of 30 keV and ion fluences of 5 × 10^{17} ion/cm^2. This work reveals a better performance of W-Ta coatings relatively to the W ones under irradiation. The behaviour is in line with previous reports arising from the irradiation of equivalent bulk materials.

Declaration of Competing Interest

The authors declare that they have no known competing financial interests or personal relationships that could have appeared to influence the work reported in this paper.

Acknowledgements

This work has been carried out within the framework of the EUROfusion Consortium, funded by the European Union via the Euratom Research and Training Programme (Grant Agreement No 101052200 - EUROfusion). Views and opinions expressed are however those of the author(s) only and do not necessarily reflect those of the European Union or the European Commission. Neither the European Union nor the European Commission can be held responsible for them. Work performed under EUROfusion WP PFC. The research leading to this result has been partially supported by Fundação para a Ciência e a Tecnologia, Portugal, through projects UID/50010/2020 and PTDC/FIS-PLA/31629/2017, by the OP VVV project CZ.02.2.69/0.0/0.0/18_053/0017163 of the Czech Academy of Sciences and by the RADIATE project under the Grant Agreement 824096 from the EU Research and Innovation programme HORIZON 2020.

References

[1] S. Nogami, I. Ozawa, D. Asami, N. Matsuta, S. Nakabayashi, S. Baumgärtner, P. Lied, K. Yabuuchi, T. Miyazawa, Y. Kikuchi, M. Wirtz, M. Rieth, A. Hasegawa, Tungsten–tantalum alloys for fusion reactor applications, J. Nucl. Mater. 566 (2022) 153740, https://doi.org/10.1016/j.jnucmat.2022.153740.

[2] Z. Wang, J. Wang, Y. Yuan, L. Cheng, S.-Y. Qin, A. Kreter, G.-H. Lu, Effects of tantalum alloying on surface morphology and deuterium retention in tungsten exposed to deuterium plasma, J. Nucl. Mater. 522 (2019) 80–85.

[3] R. Mateus, M. Dias, J. Lopes, J. Rocha, N. Catarino, P. Duarte, R.B. Gomes, C. Silva, H. Fernandes, V. Livramento, P.A. Carvalho, E. Alves, K. Hanada, J.B. Correia, Blistering of W-Ta composites at different irradiation energies, J. Nucl. Mater. 438 (2013) S1032–S1035.

[4] R. Mateus, M. Dias, J. Lopes, J. Rocha, N. Catarino, N. Franco, V. Livramento, P. A. Carvalho, J.B. Correia, K. Hanada, E. Alves, Effects of helium and deuterium irradiation on SPS sintered W-Ta composites at different temperatures, J. Nucl. Mater. 442 (1-3) (2013) S251–S255.

[5] E. Grigore, M. Gherendi, C. Hernandez, C. Desgranges, M. Firdaouss, Tungsten coatings for application in WEST project, Nucl. Mater. Energy 9 (2016) 137–140.

[6] I. Jõgi, P. Paris, K. Piip, J. Ristkok, R. Talviste, H.-M. Piirsoo, A. Tamm, E. Grigore, A. Hakola, B. Tyburska-Pueschel, H.J. van der Meiden, LIBS applicability for investigation of re-deposition and fuel retention in tungsten coatings exposed to pure and nitrogen-mixed deuterium plasmas of Magnum-PSI, Phys. Scr. 96 (11) (2021), https://doi.org/10.1088/1402-4896/ac169c.

[7] J.F. Ziegler, M.D. Ziegler, J.P. Biersack, SRIM - The stopping and range of ions in matter (2010), Nucl. Inst. Methods Phys. Res. B 268 (11-12) (2010) 1818–1823.

[8] S.J. Zenobia, L.M. Garrison, G.L. Kulcinski, The response of polycrystalline tungsten to 30keV helium ion implantation at normal incidence and high temperatures, J. Nucl. Mater. 425 (1-3) (2012) 83–92.

[9] I.-L. Velicu, V. Tiron, C. Porosnicu, I. Burducea, N. Lupu, G. Stoian, G. Popa, D. Munteanu, Enhanced properties of tungsten thin films deposited with a novel HiPIMS approach, Appl. Surf. Sci. 424 (2017) 397–406.

[10] E. Grigore, C. Ruset, M. Firdaouss, P. Petersson, I. Bogdanovic Radovic, Z. Siketic, Helium depth profile measurements within tungsten coatings by using Glow Discharge Optical Emission Spectrometry (GDOES), Surf. Coat. Technol. 376 (2019) 21–24.

[11] J.A. Maxwell, W.J. Teesdale, J.L. Campbell, The Guelph PIXE software package II, Nucl. Inst. Meth. Phys. Res. B 95 (3) (1995) 407–421.

[12] G.W. Grime, M. Dawson, Recent developments in data acquisition and processing on the Oxford scanning proton microprobe, Nucl. Instrum. Methods Phys. Res. B 104 (1-4) (1995) 107–113.

[13] T. Schwarz-Selinger, Deuterium retention in MeV self-implanted tungsten: influence of the damaging dose rate, Nucl. Mater. Energy 12 (2017) 683, https://doi.org/10.1016/j.nme.2017.02.003.

[14] N.P. Barradas, N. Catarino, R. Mateus, S. Magalhães, E. Alves, Z. Siketić, I. B. Radović, Determination of the 9Be(3He,pi)11B (i=0,1,2,3) cross section at 135° in the energy range 1–2.5MeV, Nucl. Instrum. Methods Phys. Res. Sect. B: Beam Interact. Mater. Atoms 346 (2015) 21–25.

[15] N.P. Barradas, C. Jeynes, Advanced physics and algorithms in the IBA DataFurnace, Nucl. Instrum. Methods Phys. Res. B 266 (2008) 1875–1879, https://doi.org/10.1016/j.nimb.2007.10.044.

[16] Z. Siketić, N. Skukan, I. Bogdanović Radović, A gas ionisation detector in the axial (Bragg) geometry used for the time-of-flight elastic recoil detection analysis, Rev. Sci. Instrum. 86 (8) (2015) 083301.

[17] K. Arstila, J. Julin, M.I. Laitinen, J. Aalto, T. Konu, S. Kärkkäinen, S. Rahkonen, M. Raunio, J. Itkonen, J.-P. Santanen, T. Tuovinen, T. Sajavaara, Potku – New analysis software for heavy ion elastic recoil detection analysis, Nucl. Inst. Methods Phys. Res. B 331 (2014) 34–41.

[18] Z. Zhao, et al., Effect of grain size on the behaviour of hydrogen/helium retention in tungsten: a cluster dynamics modeling, Nucl. Fusion 57 (2017), 086020, https://doi.org/10.1088/1741-4326/aa7640.

[19] V.K. Alimov, B.M.U. Scherzer, Deuterium retention and re-emission from tungsten materials, J. Nucl. Mater. 240 (1) (1996) 75–80.